



ACOUSTICS 2012

Modelling the emergence of the coherent field for cavities in a solid matrix

V. J. Pinfield and R. E. Challis

University of Nottingham, Electrical Systems and Optics Division, Faculty of Engineering,
Tower Building, University Park, Nottingham, NG7 2RD Nottingham, UK
valerie.pinfield@nottingham.ac.uk

In this paper we study the acoustic field backscattered from a plane slab of spherical scatterers. The work is motivated by the need to model the reflected field received from porous regions of composite materials when using ultrasonic NDE techniques. Here, we simulate the field received from the spherical scatterers, using a semi-analytical model for the response of single realizations of scatterer configurations, together with the coherent field for the equivalent homogeneous medium. The degree of incoherence of the simulated field response from the scatterers is calculated and its dependence on scatterer radius, concentration and frequency are determined.

1 Introduction

The investigation of the characteristics of acoustic and shear wave propagation through heterogeneous materials has been the subject of many studies and has a substantial heritage. It is well established that under certain conditions, the wave propagation appears equivalent to that in a homogeneous medium; this is termed the coherent field. The existence of a coherent field in such materials under certain conditions has been established by a variety of techniques, variously termed homogenization theories, and multiple scattering theories. Many such methods rely on an averaging process over all possible configurations of “scatterer” locations, where the “scatterer” may be cavities, inclusions etc. This averaging process is called ensemble averaging. The coherent field emerges from the summed scattered fields on application of the ensemble average. Hence the coherent field relies on sufficient averaging over many realizations of scatterer configurations.

In a measurement system, such as an NDE application, the signal received from a particular region may not be coherent, since it is a sample of a particular configuration rather than averaged over many configurations. Although averaging can be implemented at the transducer surface this may not be sufficient to result in a coherent field response. The simulations reported in this paper were designed to explore the emergence of the coherent field from the response of a planar slab of spherical scatterers. We report the conditions under which the response approaches coherence, and also demonstrate the degree of incoherence of the response and its dependence on parameters such as scatterer radius, concentration and frequency.

2 The models

The models have been reported elsewhere [1]-[2] and only a brief summary is presented here.

2.1 Discrete scatterer model

The configuration of the model is shown in Figure 1a. Spherical scatterers, each of radius a are distributed randomly in a solid homogeneous matrix in the slab region defined as shown. Scatterers are located by a random distribution as if they were point scatterers, no volume exclusion is applied. A planar transmitting and receiving device is coupled directly to the solid matrix material, and transmits a plane wave, which is assumed to be the incident wave at each scatterer. The signal received at a single point on the transducer surface is obtained from the normal displacement of the scattered fields from each scatterer, taking the far-field scattering amplitude. The amplitude and angular distribution of the scattered field are determined from the Ying and Truell formulation [3] based on the Rayleigh partial wave analysis in the long wavelength region, in order to represent the field scattered by spherical

cavities in a solid matrix. In the discrete scatterer model, there are no interfaces at front and back of the slab region, the matrix is the same material in all regions. A number of single realisations of scatterer locations are simulated using the model, with various number of scatterers and cavity radii. The volume fraction is obtained from the number density of scatterers at a particular radius.

2.2 Ensemble average model

The coherent field is obtained when an average over all possible configurations of scatterer locations is taken. This could be simulated by taking multiple simulations of the discrete scatterer model (each being a single realisation of scatterer locations) and obtaining the average scattered field. Another approximate limit is to take an integral over the scattered field using random scatterer locations approximated using a uniform probability. This approximation is possible in this case because of the assumption of an identical incident field at each scatterer, rather than taking the coherent incident field. However, the integrated solution allows us to check the limit of the discrete scatterer model.

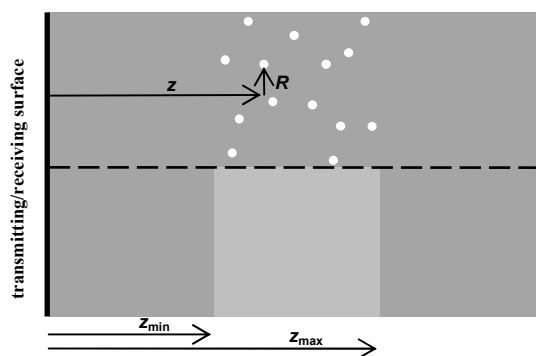


Figure 1: Configuration of system modeled (a) (above dashed line) discrete scatterer model (b) (below dashed line) effective medium model. The coordinates (z, R) of a cavity relative to the receiving point are shown.

2.3 Effective medium model

The effective medium model treats the slab region as a homogeneous material (see Figure 1b) with properties derived from homogenization or multiple scattering theories. These theories have derived the equivalent homogeneous properties of the material which gives rise to the coherent field. We use the multiple scattering theory of Foldy to obtain the wavenumber of the slab, using the scattering coefficients determined using the Ying and Truell formulation, as noted earlier. The effective density of the slab is a volume average density (using cavities). The signal received back from the slab is calculated using simple reflection and transmission coefficients, based on the

effective impedance of the slab calculated from the effective wavenumber and density.

The models attempt to simulate relatively large-scale systems, in particular the response of a plane slab region of scatterers. As such, they include simplifications such as the assumption of the simplest form of the incident field at the scatterers, and the use of the Foldy approximation for wavenumber [4]. Smaller-scale simulations such as those using finite difference methods, are able to use higher order approximations but are constrained to a much smaller length scale [5]-[6]. In the current calculations, the response is observed at a single point on the receiving surface, to remove any effects of receiver area averaging.

2.4 Numerical calculations

Calculations were carried out in Matlab, using the parameter set given in Table 1. The solid matrix was assigned properties typical of an averaged fibre/resin composite; longitudinal sound speed 3035 ms^{-1} , density 1564 kg m^{-3} and shear modulus 3.6 GPa . Simulations were carried out in the frequency domain, using a sampling frequency of 50 MHz with 1024 samples. In order to produce time-domain results, the response of a transmitter-receiver pair of 10 MHz centre-frequency transducers was measured in pitch-catch configuration in water. A simulated 5 MHz centre-frequency signal was produced by sub-sampling that measured signal. Table 1 shows the cavity radii used in the simulations, from $5\text{-}20 \text{ }\mu\text{m}$, and the corresponding number of cavities in the simulated region at 20% concentration. It should be noted that in each simulation all cavities have the same radii. Although the simulation aims to represent a planar slab of scatterers, the region must be limited in the radial dimension R (see Figure 1a). Test showed that $R_{\text{max}}=20 \text{ mm}$ was sufficient to represent the response of the full plane. All effective medium calculations were carried out at 1% by volume of cavities. Discrete scatterer model results were first scaled by concentration in order to compare them with the effective medium results. Frequency domain results were also smoothed by windowing in the time-domain. Fuller details of the simulations are given in [1]-[2].

Table 1: System parameters.

Distance z_{min} / mm	2
Layer thickness / mm	1
Cavity conc / v/v%	1,2,5,10,20
Cavity radius / μm	5.0, 7.9, 10.0, 15.9, 20.0
Millions of cavities at 20 v/v% (respectively with radius)	480, 120, 60, 15, 7.5

3 Results

3.1 Time-domain results

The signal received from the scatterers in a single realization, according to the discrete scatterer model, is

shown in Figure 2 (in black), together with the coherent field obtained from the effective medium model (in red). The simulations were for a cavity radius of $10 \text{ }\mu\text{m}$ at $2\%\text{v/v}$ (plotted results are scaled by concentration) with a 10 MHz centre-frequency signal. In these conditions the received field shows a high degree of incoherence, with little similarity to the coherent field, with its reflected signals from the front and back of the layer. However, under different conditions, using $5 \text{ }\mu\text{m}$ radius cavities at $10\%\text{v/v}$ concentration, and with a 5 MHz centre-frequency signal (Figure 3) the discrete scatterer response is almost identical to the coherent field.

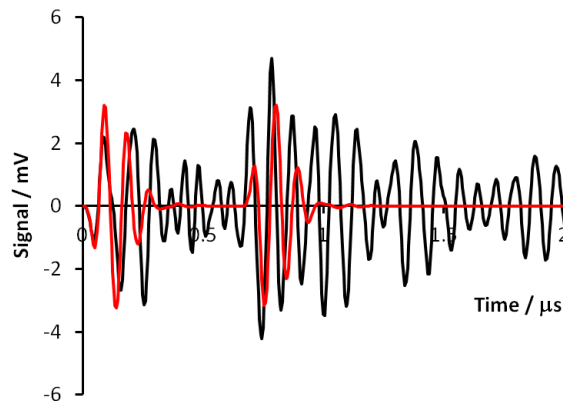


Figure 2: Time-domain results for discrete scatterer model (black) and effective medium model (red) for $10 \text{ }\mu\text{m}$ radius cavities at $2\%\text{v/v}$ with a 10 MHz centre-frequency signal (scaled by concentration).

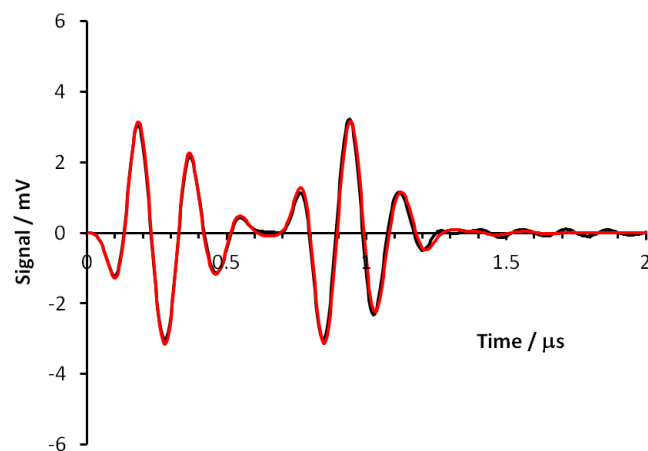


Figure 3: Time-domain results for discrete scatterer model (black) and effective medium model (red) for $5 \text{ }\mu\text{m}$ radius cavities at $10\%\text{v/v}$ with a 5 MHz centre-frequency signal (scaled by concentration).

3.2 Frequency-domain results

Although the degree of coherence is readily observed in time-domain plots, more information is obtained from frequency-domain data. The results of each model are plotted against frequency for a cavity radius of $10 \text{ }\mu\text{m}$ in Figure 4 (scaled by concentration). The coherent field calculated from the effective medium model shows the resonant behavior typical of the response from a layer, and is in close agreement with the integrated ensemble average field. The discrete scatterer results are shown for a concentration of 5% (scaled by concentration), and compared with the effective medium and ensemble average

results at 1% concentration. At low frequencies, the single realization represented by the discrete scatterer model produces almost identical backscattered signal to the effective medium and ensemble average limits. Hence, even for a single realization of a planar slab of scatterers, at low frequencies the backscattered field approaches the coherent field. At higher frequencies, the discrete scatterer model deviates increasingly from the coherent field.

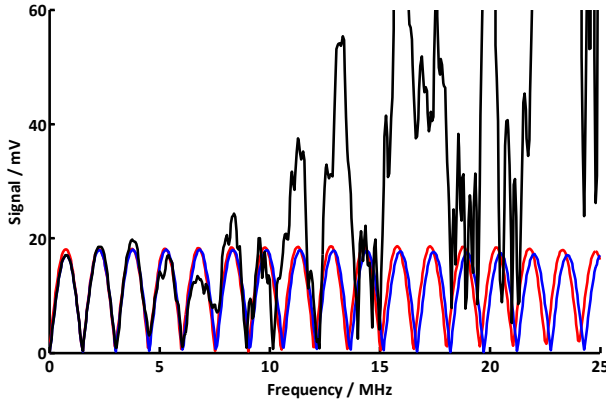


Figure 4: Frequency-domain results for discrete scatterer model (black) at 5% concentration (scaled), effective medium model (red), and integrated ensemble average model (blue) for 10 μm radius cavities at 1%v/v.

3.3 Deviation from coherence

The deviation of the response of the discrete scatterer model from the coherent field was calculated by using the sum of the squared residuals (RSS) between the two model responses (having scaled the discrete scatterer response by concentration). The RSS value was calculated up to each frequency in turn, giving a result as a function of bandwidth or maximum frequency. Figure 5 shows the RSS plotted against frequency (or bandwidth) for various radius/concentration pairs. The plot indicates that there are systematic variations in the deviation from coherence with both radius and concentration, and that the deviation (as quantified by the RSS) increases with frequency.

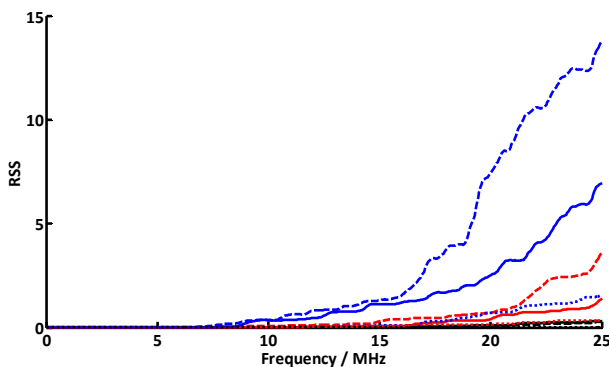


Figure 5: Sum of the squared residuals of a single realization of the discrete scatterer model compared with the effective medium model for selected cavity radius and concentration. Lines styles denote 1% (dashed), 2% (solid), and 10% (dotted) concentration. Colours denote 5 μm (black), 10 μm (red) and 15.9 μm (blue).

3.4 Incoherence with lengthscale

The criterion for the emergence of the coherent field from a single realization of scatterers is related to the principal length scaling in the system. If the controlling length parameter is denoted by q then coherence is expected to be obtained when $q/\lambda \ll 1$, that is, where the wavelength is much longer than the length scale in the system [7]. For distributed spherical scatterers, we expect the relevant lengthscale to be related to the average distance between particles, since it represents the lengthscale of the heterogeneity. We take this length to be

$$l = r/\phi^{1/3} \quad (1)$$

We rescale the results for the deviation of the single realization response from coherence (using RSS) as a function of the parameter l/λ , shown in Figure 6. All of the frequency, radius and concentration dependence is now incorporated into the dimensionless length ratio. However, some systematic dependencies on radius and concentration remain, since the curves do not reduce to a single line. Although the quantity of data means not all curves can be distinguished visually in Figure 6, the systematic variations can be detected. This implies that the parameter l/λ does not account fully for the degree of incoherence of the response. Some spread in the curves is still to be expected since each represents the response of one single realization at the given radius and concentration; different realizations for the same radius and concentration will produce different responses. However, we expect to remove all *systematic* variation with these variables.

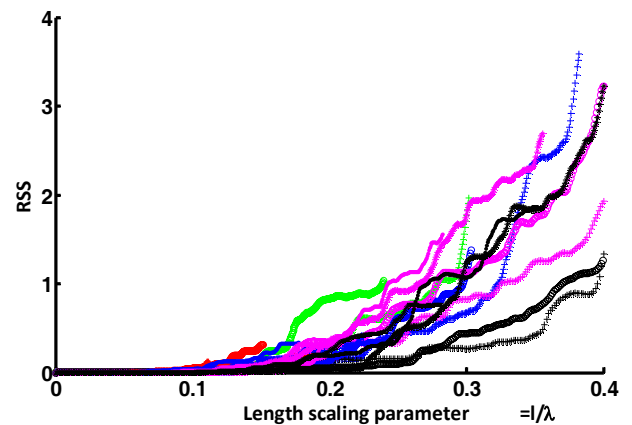


Figure 6: RSS plotted against length scale parameter l/λ for all sets of radii and concentration for the discrete scatterer model single realizations. Radii [5,7,9,10,15,9,20 μm] are denoted by colours in sequence [red, green, blue, magenta, black] and symbols [+ , \circ , * , . , x] denote concentrations [1,2,5,10,20%].

A fitting process was carried out, as described in [2], to determine the relationship between the variables. A cut-off value for RSS was chosen based on the apparent coherence condition for various radii and concentrations in the time domain with the two centre frequencies of 5, 10 MHz. The frequency, radius and concentrations at this value of RSS were fitted to power law dependencies, resulting in a relationship which indicated the parameter

$$\left(l^{2/3}\right)/\lambda \quad (2)$$

as determining the relevant scaling. This is no longer a dimensionless parameter; and the units of length were taken in microns. Replotting the RSS data for the full frequency range against this new scaling parameter results in a considerably narrower spread of data, shown in Figure 7. Although some spread remains in the data, the obvious systematic trends have been removed, which is particularly clear for the different colours denoting the various radii. The remaining spread may be due to the differences between individual realizations with the same radius and concentration. This is evidenced by plotting the mean of multiple simulations at the same conditions, which results in a very narrow spread of curves when using the parameter in Eq. (2) (not shown here). The variation in the degree of incoherence for the same radius and concentration will be explored in a further publication.

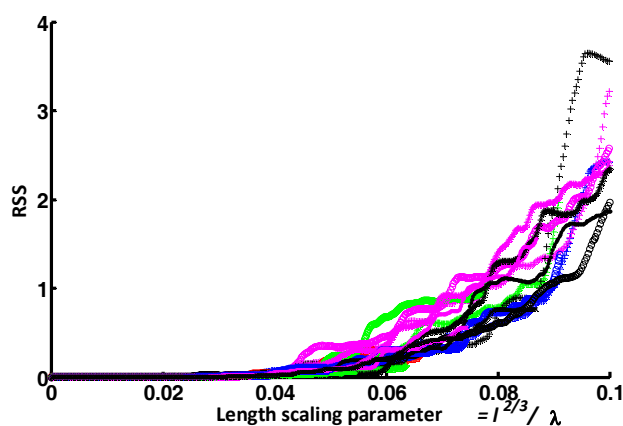


Figure 7: RSS plotted against length scale parameter $l^{2/3}/\lambda$ (micron units) for all sets of radii and concentration for the discrete scatterer model single realizations. The legend is identical to Figure 6

Our results indicate that our measure of incoherence (RSS) cannot be accounted for solely by the relative size of the wavelength compared with a length scale parameter based on the mean distance between scatterers. There are a number of possible explanations for this. Firstly, this measure of incoherence may not relate linearly to a more rigorous mathematically-defined degree of incoherence. Secondly, there may be other relevant length scales in the system which contribute to incoherence, but which are not included in the analysis, or are constant in all simulations. According to our fitting results, the mean distance between particles accounts only partially for the degree of incoherence.

5 Conclusion

Simulations of the response of single realizations of spherical scatterers (cavities) in a slab have been used to demonstrate the emergence of the coherent field in such cases. The degree of incoherence was found to increase with increasing radius, decreasing concentration, and increasing frequency. This is consistent with the requirement that the wavelength should be much longer than the relevant length scale of the system, assumed to be

the mean distance between scatterers. However, fitting a measure of the degree of incoherence to the parameter set has suggested that the mean distance between particles only partially accounts for the incoherence.

References

- [1] V. J. Pinfield, R. E. Challis and R. A. Smith, "A comparison of stochastic and effective medium approaches to the backscattered signal from a porous layer in a solid matrix," *J. Acoust. Soc. Am.* 130 (1), 122-134 (2011)
- [2] V. J. Pinfield and R. E. Challis, "Simulation of incoherent and coherent backscattered response of cavities in a solid matrix," submitted to *J. Acoust. Soc. Am.* (2012)
- [3] C. F. Ying and R. Truell, "Scattering of a plane longitudinal wave by a spherical obstacle in an isotropically elastic solid," *J. Appl. Phys.* 27, 1086-1097 (1956)
- [4] L. L. Foldy, "The multiple scattering of waves," *Phys. Rev.* 67 (3-4), 107-119 (1945)
- [5] B. Galaz, G. Haiat, R. Berti, N. Taulier, J. J. Amman and W. Urbach, "Experimental validation of a time domain simulation of high frequency ultrasonic propagation in a suspension of rigid particles," *J. Acoust. Soc. Am.* 127 (1), 148-154 (2010)
- [6] J. Dubois, C. Aristegui, O. Poncelet and A. L. Shuvalov, "Coherent acoustic response of a screen containing a random distribution of scatterers: comparison between different approaches," *J. Phys: Conf. Ser.* 269, 012004 (2011)
- [7] W. J. Parnell and I. D. Abrahams, "A new integral equation approach to elastodynamic homogenization," *Proc. Roy. Soc. A* 464 (2094), 1461-1482 (2008)